

# Supporting Information

Uchida et al. 10.1073/pnas.1117537109

## SI Materials and Methods

For microarray and statistical analysis, developing inflorescence tips from 33-d-old WT Col, *er-2*, and *epfl4 epfl6/chal-2* were subjected to RNA preparation, cDNA synthesis, and hybridization to Affymetrix ATH1 chips. *er-2* was used because *er-105* carries an additional *gll* mutation (1). Three biological replicates were used. The microarray data were normalized as described previously (2). Quality control and RMA normalization with Benjamin-Hochberg *P* value correction was performed using Robin software (3). Further statistical analysis was performed using MultiExperiment Viewer software (4). Genes with statis-

tically significant (*Q* value cutoff of <0.001) deregulation compared with WT were identified using the Significance of Microarrays module. A twofold-change filter was applied as a cutoff. Annotation of genes and classification into functional pathways was performed with MapMan software (5). PageMan software (6) was used for overrepresentation analysis. Overrepresentation of promoter motifs in commonly regulated genes was performed with the Analysis Suite of the Athena tool (<http://www.bioinformatics2.wsu.edu/athena>), using a *P* value cutoff of 0.001. A distance 3,000 bp upstream of genes was considered with cutoffs at adjacent genes activated.

1. Torii KU, et al. (1996) The *Arabidopsis* *ERECTA* gene encodes a putative receptor protein kinase with extracellular leucine-rich repeats. *Plant Cell* 8:735–746.
2. Pillitteri LJ, Peterson KM, Horst RJ, Torii KU (2011) Molecular profiling of stomatal meristemoids reveals new component of asymmetric cell division and commonalities among stem cell populations in *Arabidopsis*. *Plant Cell* 23:3260–3275.
3. Lohse M, et al. (2010) Robin: An intuitive wizard application for R-based expression microarray quality assessment and analysis. *Plant Physiol* 153:642–651.
4. Saeed AI, et al. (2003) TM4: A free, open-source system for microarray data management and analysis. *Biotechniques* 34:374–378.
5. Thimm O, et al. (2004) MapMan: A user-driven tool to display genomics data sets onto diagrams of metabolic pathways and other biological processes. *Plant J* 37:914–939.
6. Usadel B, et al. (2006) PageMan: An interactive ontology tool to generate, display, and annotate overview graphs for profiling experiments. *BMC Bioinformatics* 7:535.

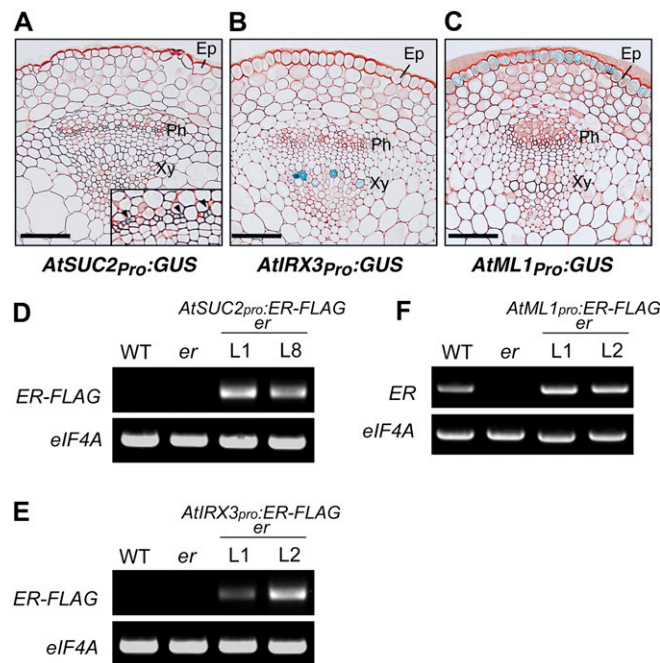


**Fig. S1.** Activities and expression patterns of tissue layer-specific promoters used in this study. (A–C) Reporter  $\beta$ -glucuronidase (GUS) histochemical analysis. Shown are inflorescence stem sections from transgenic *Arabidopsis* plants expressing *AtSUC2pro:GUS* (A), *AtIRX3pro:GUS* (B), and *AtML1pro:GUS* (C). Specific GUS staining detected in the phloem (companion cells; A), xylem (B), and epidermis (C) indicate that the three promoter fragments used in this study drive correct expression patterns. (Scale bar: 25  $\mu$ m.) (D–F) Expression of *ER-FLAG* transcripts driven by tissue-specific promoters. Shown is the RT-PCR analysis of *ER-FLAG* (D and E) and *ER* transcripts (F) from seedlings of WT, *er*, and two transgenic *er* lines each expressing *AtSUC2pro:ER-FLAG* (D), *AtIRX3pro:ER-FLAG* (E), and *AtML1pro:ER-FLAG* (F). For D and E, a reverse primer corresponding to the C-terminal FLAG-tag region was used for PCR, resulting in the absence of transcripts in WT (nontransgenic plants). *eIF4A* expression served as a positive control.

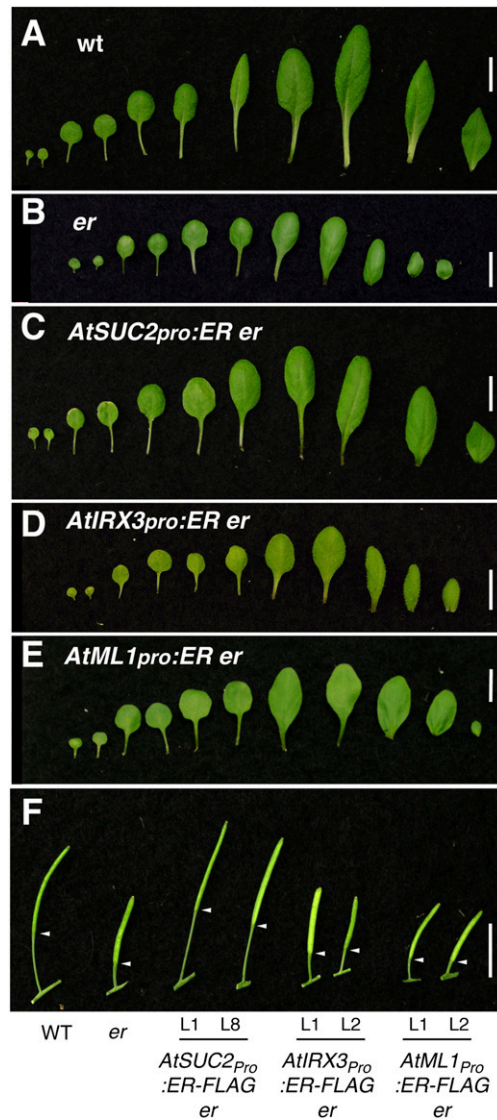


**Fig. S2.** Leaf and silique phenotypes of *er* plants expressing ERECTA-FLAG driven by the tissue layer-specific promoters. (A–E) Leaves (cotyledons, rosette leaves, and cauline leaves) from 4-wk-old *Arabidopsis* of WT (A), *er-105* (*er*) (B), and transgenic *er* plants expressing *AtSUC2pro:ER-FLAG* (C), *AtIRX3pro:ER-FLAG* (D), and *AtML1pro:ER-FLAG* (E). Leaves were dissected from the primary shoot axis and laid out in the sequence of development (left, base; right, apex). (Scale bars: 10 mm.) (F) Fully expanded siliques from WT, *er-105* (*er*), and transgenic *er* plants expressing *AtSUC2pro:ER-FLAG*, *AtIRX3pro:ER-FLAG*, and *AtML1pro:ER-FLAG*. (Scale bar: 10 mm.) The phloem-specific expression of *ER* rescues leaf and silique elongation defects of *er*.



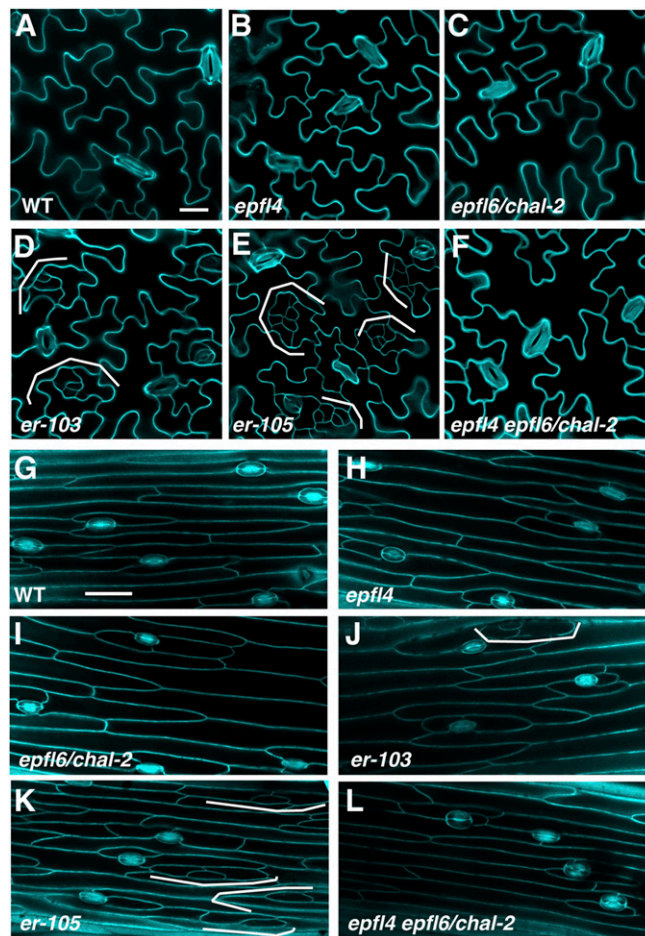


**Fig. S4.** *epfl4 epfl6/chal-2* mutant does not exhibit stomatal patterning defects like *er*. (A–F) Two-wk-old cotyledon abaxial epidermis from WT (A), *epfl4* (B), *epfl6/chal-2* (C), *er-103* (D), *er-105* (E), and *epfl4 epfl6/chal-2* (F). (G–L) Six-wk-old inflorescence stem epidermis from WT (G), *epfl4* (H), *epfl6/chal-2* (I), *er-103* (J), *er-105* (K), and *epfl4 epfl6/chal-2* (L). *er* mutant cotyledon and stem epidermis exhibits characteristic phenotype of excessive asymmetric entry divisions, leading to clusters of small, stomatal-lineage ground cells with an arrested stomatal precursor (brackets). The null allele *er-105* (E and K) shows more a severe phenotype than the intermediate allele *er-103* (D and J). Unlike in *er*, the epidermis of *epfl4 epfl6/chal-2* double mutant (F and L) does not undergo aberrant, excessive asymmetric entry divisions. A–F were obtained under the same magnification, as were G–L. (Scale bars: 20  $\mu$ m.)

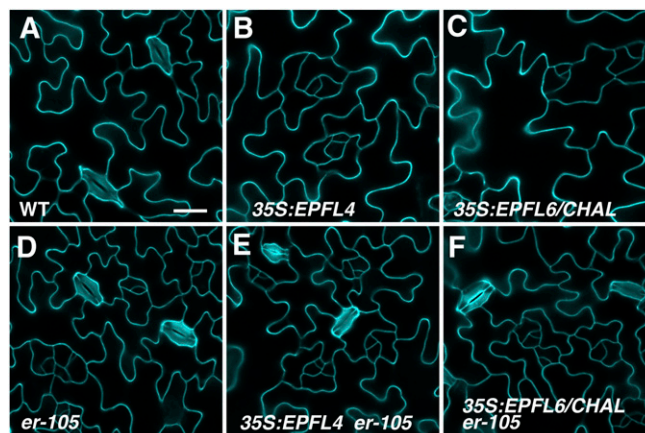


**Fig. S5.** Ectopic overexpression of *EPFL4* and *EPFL6/CHAL* in an *er* null background. Shown are 2-wk-old cotyledon abaxial epidermis from WT (A), *CaMV35S:EPFL4* (B), *CaMV35S:EPFL6/CHAL* (C), *er-105* (D), *CaMV35S:EPFL4* in *er-105* (E), and *CaMV35S:EPFL6/CHAL* in *er-105* (F). Ectopic overexpression of *EPFL4* and *EPFL6/CHAL* (B and C) inhibits stomatal differentiation, resulting in arrested precursors. The ectopic effects are diminished in the absence of *ER* (E and F). All images were obtained under the same magnification. (Scale bar: 20  $\mu$ m.)

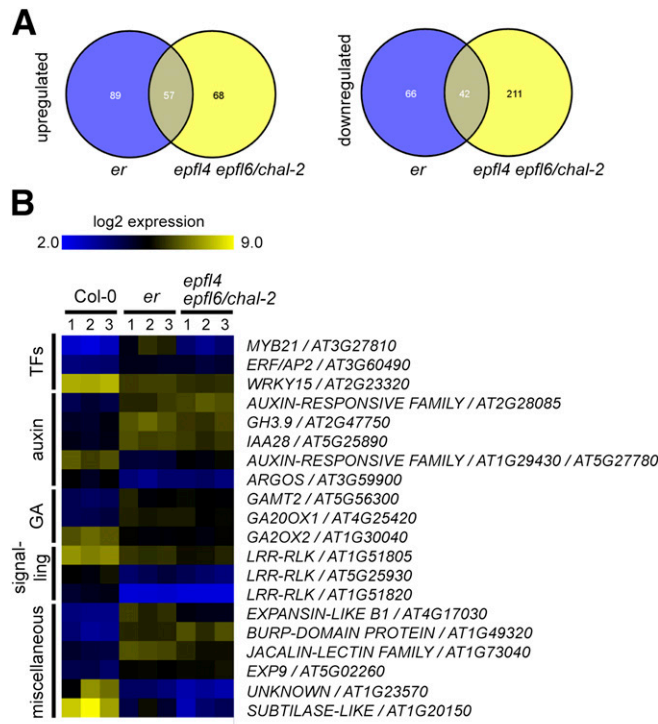


**Fig. S6.** Molecular profiling of *er* and *epfl4 epfl6* inflorescences reveals a set of commonly regulated genes. (A) Venn diagram depicting the number of genes commonly up-regulated and down-regulated in *er* and *epfl4 epfl6/cha1-2*. (B) Heat map representation depicting up-regulation or down-regulation of each indicated gene in *er* or *epfl4 epfl6/cha1-2* compared with WT. Three replicates are shown to demonstrate consistency. The scale represents log<sub>2</sub>-transformed expression values. Genes are grouped according to functional classification.

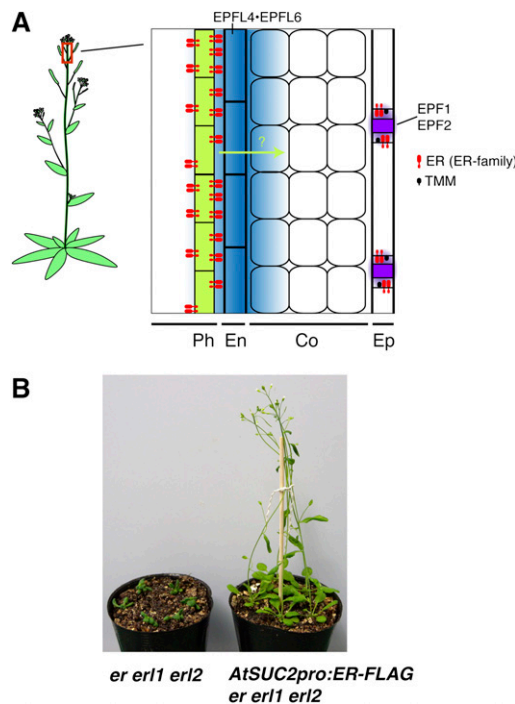


**Fig. S7.** Endodermis–phloem cell–cell communication mediated by EPFL4/6 and ERECTA specifies inflorescence architecture. (A) Schematic diagram. Proper inflorescence stem and pedicel elongation is mediated by EPFL4 and EPFL6, two peptides (blue) expressed and secreted from the endodermis (En) to neighboring tissues. Plasma membrane-localized ER (red) in the adjacent phloem tissue (Ph, light green) perceives EPFL4/6. EPFL4/6-ER signaling promotes cortex cell proliferation in inflorescence in a non-cell autonomous manner by an unknown factor (arrow). ER is also expressed in the epidermis (Ep), where it receives EPF1/2 (purple) from stomatal precursor cells and restricts stomatal density. The leucine-rich repeat receptor-like protein TOO MANY MOUTHS (black) is specifically expressed in the epidermis and modulates ER activity. No similar receptor-like protein in the phloem is known. (B) Phloem-specific expression of ER is sufficient to fully rescue the severe dwarf phenotype of *er erl1 erl2* triple-mutant plants. Shown are 4-wk-old plants of WT, *er erl1 erl2*, and *AtSUC2pro:ER-FLAG* in *er erl1 erl2*.

	10	20	30	40	50	
At4g37810_EPFL2	IGSRPPRCERVRCRSCG-HCEAIQVPT--NPQTKLHSPLTTSSSSSSETI					[ 47 ]
At5g10310_EPFL1	LGSTPPSCH-NRCNNCH-PCMAIQVPT-LPTRSRFTRVNPFGGFFVRPPS					[ 47 ]
At1g80133_EPFL8	MGSEPPVCA-TKCRNCK-PCLPYLFDIRGAHDDDDDDSEF-----					[ 37 ]
At2g30370_EPFL6	LGSSPPRCS-SKCGRCT-PCKPVHVPVPP--GTPVTAE-----					[ 34 ]
At3g22820_EPFL5	PGSVPPMCR-LKCGKCE-PKAVHVP IQP--GLIMPLE-----					[ 34 ]
At4g14723_EPFL4	PGSSPPTCR-SKCGKCE-PCKPVHVP IQP--GLSMPLA-----					[ 34 ]
AB499312_EPFL3	IGSKPPSCE-KKCYGCE-PCEAIQVPTISSIPHLSPHYA-----					[ 37 ]
At4g12970_EPFL9	IGSTAPTCTYNECRGCRYKRAEQVPEG--NDPINS-----					[ 35 ]
At2g20875_EPF1	AGSRLPDCS-HACGSCS-PCRLVMVSFVCASVE--EAETC-----					[ 36 ]
At1g34245_EPF2	TGSSLPDCS-YACGACS-PCKRVMISFECS-----VAESC-----					[ 33 ]
AB499313_EPFL7	SGSSIPDCS-NACGPCK-PCKLVVISSTCS-----ASEAC-----					[ 33 ]
	60	70	80			
At4g37810_EPFL2	HLDYTRGDDSTNYKPMWKCCKGNSIYNP----					[ 76 ]
At5g10310_EPFL1	SLTTVLQDQYS-NYKPMGWKCHCNGHFYNP----					[ 75 ]
At1g80133_EPFL8	-----YYPVKWICRCRDRVFEP----					[ 54 ]
At2g30370_EPFL6	-----YYPEAWRCKCGNKLMP----					[ 51 ]
At3g22820_EPFL5	-----YYPEAWRCKCGNKLMP----					[ 51 ]
At4g14723_EPFL4	-----YYPEAWRCKCGNKLMP----					[ 51 ]
AB499312_EPFL3	-----NYQPEGWRCHCPPP-----					[ 51 ]
At4g12970_EPFL9	-----AYHYRCVCHR-----					[ 45 ]
At2g20875_EPF1	-----PMAYKCMCNKSYVVP----					[ 52 ]
At1g34245_EPF2	-----SVIYRCTCRGRYHVPSRA [ 52 ]					[ 52 ]
AB499313_EPFL7	-----PLVYKCLCKGKYHVPSLT [ 52 ]					[ 52 ]

Fig. S8. Amino acid sequence alignment of the EPFL family genes used in this study. The predicted mature C-terminal EPF/EPFL domains were used for the alignment. The alignment was generated using Clustal X GUI version (<http://www.clustal.org/download/current/>).

## Other Supporting Information Files

[Dataset S1 \(XLS\)](#)